Journal of Molecular Structure 1083 (2015) 39–47

Contents lists available at ScienceDirect

Journal of Molecular Structure

journal homepage: www.elsevier.com/locate/molstruc

NMR, FT-IR, FT-Raman, UV spectroscopic, HOMO–LUMO and NBO analysis of cumene by quantum computational methods

T. Sivaranjani [a,*], S. Xavier [a,b], S. Periandy [c]

[a] Bharathiyar University, Coimbatore, Tamilnadu, India
[b] Department of Physics, St. Joseph College of Arts and Science, Cuddalore, Tamil Nadu, India
[c] Department of Physics, Tagore Arts College, Puducherry, India

HIGHLIGHTS

- The compound isopropyl benzene (cumene) has been investigated using FT-IR, FT-Raman and NMR and UV–Vis spectroscopic tool.
- The chemical shift of the compounds is found and it is favour for its change of chemical property.
- The stable geometry of the molecule through conformational study is carried out.
- The charge transfer in the molecule by HOMO–LUMO studied in relation with NBO analysis.

GRAPHICAL ABSTRACT

The isopropyl benzene (cumene) is an aromatic organic compound and is extensively studied due to its wide applications in biomedical and industrial fields. Considering its industrial and biomedical importance, a thorough analysis of physical and chemical properties is made for this molecule. It will be a helpful source to enrich the knowledge in the field of biomedical industries.

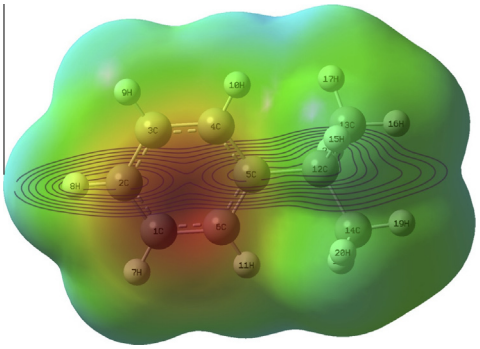

ARTICLE INFO

Article history:
Received 31 May 2014
Received in revised form 15 November 2014
Accepted 15 November 2014
Available online 21 November 2014

Keywords:
Cumene
Chemical shifts
Phenol
HOMO–LUMO

ABSTRACT

This work presents the investigation of cumene using the FT-IR, FT-Raman, NMR and UV spectra obtained through various spectroscopic techniques. The theoretical vibrational frequencies and optimized geometric parameters have been calculated by using HF and density functional theory with the hybrid methods B3LYP, B3PW91 and 6-311+G(d,p)/6-311++G(d,p) basis sets. The theoretical vibrational frequencies have been scaled and compared with the corresponding experimental data. ^{1}H and ^{13}C NMR spectra were recorded and chemical shifts of the molecule were compared to TMS by using the Gauge-Independent Atomic Orbital (GIAO) method. A study on the electronic and optical properties, absorption wavelengths, excitation energy, dipole moment and frontier molecular orbital energies, and potential energy surface (PES) is performed using HF and DFT methods. The thermodynamic properties (heat capacity, entropy and enthalpy) at different temperatures are also calculated. NBO analysis is carried out to picture the charge transfer between the localized bonds and lone pairs. NLO properties related to polarizability and hyperpolarizability are also discussed.

* Corresponding author. Tel./fax: +91 9443428971.
E-mail address: ranjanimec@gmail.com (T. Sivaranjani).

http://dx.doi.org/10.1016/j.molstruc.2014.11.035
0022-2860/

Introduction

The other name of cumene is isopropyl benzene (ISPB) which consists aromatic hydrocarbon with aliphatic substitution. Benzene is converted to isopropyl benzene (cumene) by treatment with propylene and acidic catalyst.

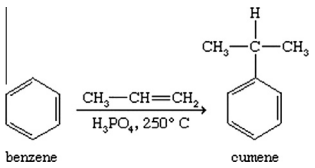

Based on the simple aromatic structure it is generally assumed that under aerobic conditions isopropyl benzene is bio-degraded. But presence of the isopropyl moiety with the phenyl ring hinders microbial oxidation which results in lower degradation. Cumene undergoes oxidation to give cumene hydro peroxide. By the catalytic action of dilute sulphuric acid, cumene hydro peroxide is split into phenol and acetone [1]. Phenol in its various formaldehyde resins to bond construction materials like plywood and composition board (40% of the phenol produced) for the bisphenol A. It is also employed in making epoxy resins and polycarbonate (30%) and for caprolactam and also as starting material for nylon (20%). Cumene is also used in minor amount as a thinner for paints, enamels and lacquers [2].

A vibrational study and structural study have been carried out by Fishman et al. [9] in *ab initio* and normal coordinate analysis. Spectra of cumene and other alkyl benzenes, obtained with the help of the Time of Flight Mass Spectroscopy (TOFMS) technique were investigated in [3]. Lagowski et al. and Schaefer et al. [4,5] have made study on the theoretical simulations of molecule on the conformation study for the molecule and obtained two conformers at minimum energies 14.5 kJ/mol and 13.4 kJ/mol. In the present study a complete theoretical and spectroscopic investigation of ISPB are carried out which were not performed in the previous works.

Experimental details

The FTIR, FT Raman and FT NMR compound under investigation namely were obtained from M/S Aldrich Chemicals, USA. According to the report, the FT-IR spectrum of the compound was recorded in Perkin–Elmer 180 spectrometer between 4000 and 400 cm^{-1} with the spectral resolution is ±2 cm^{-1}. The FT-Raman spectrum of the compound was recorded in the same instrument with FRA 106 Raman module equipped with Nd:YAG laser source operating at 1.064 μm line widths with 200 mW powers. The frequencies of all sharp bands are accurate to ±1 cm^{-1}. The high resolution H NMR and C NMR spectra were recorded using 300 MHz and 75 MHz NMR spectrometer respectively. The UV–Vis spectra were recorded in liquid phase dissolved in ethanol in the range of 200–400 nm, with the scanning interval of 0.2 nm, using the UV-1700 series instrument.

Computational methods

The entire quantum chemical calculations are performed on a Pentium IV/3.02 GHz personal computer using the Gaussian 09 software programs [6]. The calculated frequencies are scaled by suitable scale factors. The wave numbers and the geometry of the title molecule ISPB are computed using B3LYP functional and 6-311+G(d,p) [7] basis set and the same geometry is used for the conformational analysis using semi-empirical method and PM6 basis set. The electronic properties, such as NBO and HOMO–LUMO were calculated using time-dependent TD-SCF – B3LYP method under the same basis set. Similarly the NMR chemical shifts are also carried out by GIAO method in combination with B3LYP/6-311G+(2d,p). In addition, the dipole moment, linear polarizability and the first order hyper polarizability of the title molecule are also computed using B3LYP method with the 6-311+G(d,p) basis set. The optimized structure of the molecule is shown Fig. 1.

Results and discussion

Potential energy surface (PES) scan

The conformational analysis of the molecule ISPB was performed by the potential energy surface (PES) scan function with the B3LYP/6-31++G(d,p) basis set by varying the dihedral angel 5C—12C—14C—18H in steps of 18° over one complete rotation 0–360 as recommended in the similar work [8]. The graphical result, total energy versus scan coordinate, of this conformer is presented in Fig. 2. The graph clearly shows that there are three minimum conformer at 60°, 180° and 300° with same energy 3.649×10^{-23} kJ/mol. By which all these three conformers with the same minimum energy are the stable conformer of the compound.

The minimum energies obtained by the present study are much lower than the similar previous study by Fishman et al. [9]. The difference is due to usage of higher basis set in the present study which includes the corrected correlation in the many body system.

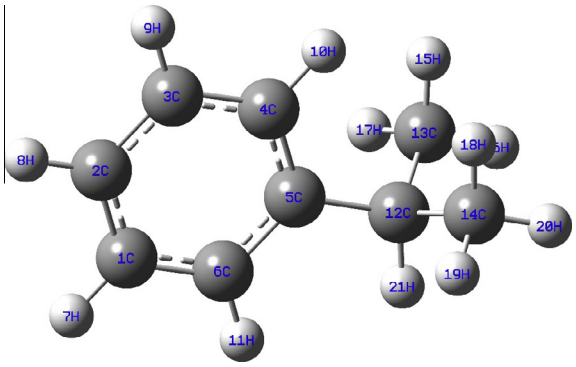

Fig. 1. Optimized structure of cumene.

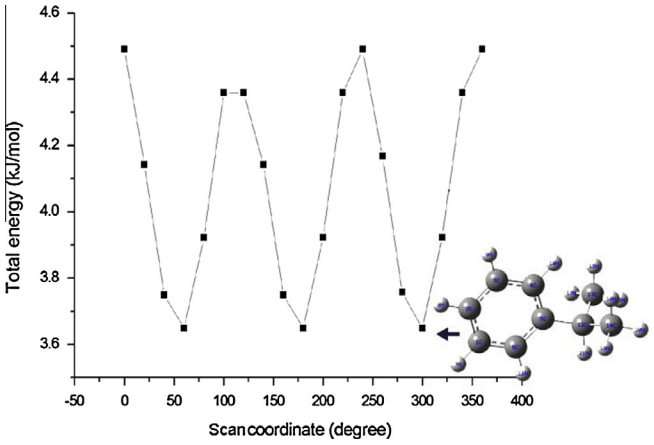

Fig. 2. Potential surface energy graph of cumene (dihedral angle –5C–12C–14C–18H).

Table 1
Optimized geometrical parameter for isopropyl benzene (cumene) using HF, B3LYP & B3PW91/6-31++G(d,p).

Geometrical parameters	Methods			Experimental value
	HF	B3LYP	B3PW91	
	6-31++G(d,p)	6-31++G(d,p)	6-31++G(d,p)	
Bond length (Å)				
C1—C2	1.38	1.39	1.39	
C1—C6	1.38	1.39	1.39	
C1—H7	1.07	1.08	1.08	
C2—C3	1.38	1.39	1.39	
C2—H8	1.07	1.08	1.08	
C3—C4	1.38	1.39	1.39	1.397
C3—H9	1.07	1.08	1.08	
C4—C 5	1.39	1.40	1.40	1.394
C4—H10	1.07	1.08	1.08	
C5—C6	1.39	1.40	1.40	1.396
C5—C12	1.53	1.53	1.52	
C6—H11	1.07	1.08	1.08	
C12—C13	1.53	1.54	1.53	
C12—C14	1.53	1.54	1.53	
C12—H21	1.09	1.10	1.10	
C13—H15	1.08	1.09	1.09	
C13—H16	1.08	1.09	1.09	
C13—H17	1.08	1.09	1.09	
C14—H18	1.08	1.09	1.09	
C14—H19	1.08	1.09	1.09	
C14—H20	1.08	1.09	1.09	
Bond angle (degree)				
C2—C1—C6	120	120	120	120.1
C2—C1—H7	120	120	120	
C6—C1—H7	119	119	119	
C1—C2—C3	118	118	118	
C1—C2—H8	120	120	120	
C3—C2—H8	120	120	120	
C2—C3—C4	120	120	120	119.4
C2—C3—H9	120	120	120	
C4—C3—H9	119	119	119	
C3—C4—C5	121	121	121	
C3—C4—H10	118	118	118	
C5—C4—H10	120	120	120	
C4—C5—C6	117	117	117	
C4—C5—C12	121	121	121	
C6—C5—C12	121	121	121	
C1—C6—C5	121	121	121	
C1—C6—H11	118	118	118	
C5—C6—H11	120	120	120	
C5—C12—C13	113	113	113	
Dihedral angle (degree)				
C6—C1—C2—C3	0.08	0.02	0.01	
C6—C1—C2—H8	−179	−179	−179	
H7—C1—C2—C3	−179	179	179	
H7—C1—C2—H8	0.05	0.01	0.0	
C2—C1—C 6—C5	0.02	0.00	−0.0	
C2—C1—C6—H11	−179	179	179	
H7—C1—C6—C5	−179	−179	−179	
H7—C1—C6—H11	0.10	0.09	0.05	
C1—C2—C3—C4	−0.08	−0.02	−0.01	
C1—C2—C3—H9	179	−179	−179	
H8—C2—C3—C4	179	179	179	
H8—C2—C3—H9	−0.05	−0.01	−0.0	
C2—C3—C4—C5	−0.02	−0.00	0.0	
C2—C3—C4—H10	179	−179	−179	
H9—C3—C4—C5	179	179	179	
H9—C3—C4—H10	−0.10	−0.09	−0.0	
C3—C4—C5—C6	0.13	0.04	−0.0	
C3—C4—C5—C12	177	177	177	

Molecular geometry

The optimized structure of the molecule is obtained from Gaussian 09 and Gauss view program [9]. The internal coordinates describe the position of the atoms in terms of distances, angles and dihedral angles with respect to an origin. The optimized bond lengths and bond angles of this compound are calculated by HF, B3LYP and B3PW91 methods with 6-31++G(d,p) basis set are listed in Table 1. This molecule has nine C—C and twelve C—H bond lengths. The C3—C4 bond distance calculated by HF/6-31++G(d,p) is 1.387 B3LYP/6-31++G(d,p) is 1.397 and B3PW91/6-31++G(d,p) is 1.395. By comparing these values with experimental value of 1.397 Å, it is observed that B3LYP estimate better the C—C bond length than HF and B3PW91. The carbon–carbon bonds in benzene

ring are not of the same length, however, the differences between the six C—C distances are small. The optimized bond lengths of C1—C2, C2—C3, C5—C6, C1—C6 and C5—C4 are 1.396, 1.385, 1.395, 1.3975 and 1.395 for B3LYP/6-311+G(d,p) method, which are in quite good agreement with experimental data.

The bond angle in the benzene ring is expected to be almost equal to 120°, but due to the substitution of the methyl groups at the point of substitution, the angle C4—C5—C6 (118.86°) and C1—C2—C3 (117.06°) are shortened. The angles C4—C5—C12, C6—C5—C12, C1—C6—C5 are found to be same with 121°, this elongation is also due to the distortion of the benzene ring by the substitution. The angles C5—C12—C13, C5—C12—H21, C13—C12—C14, and H15—C13—H17 are 113°, 106°, 109° and 107° respectively, these are angles between the carbon atoms in the substitution methyl group which clearly shows that they are not hexagonal like in benzene ring.

Molecular electrostatic potential

Molecular electrostatic potential for stable conformer calculated at B3LYP/6-31+G(d,p) level for the optimized geometry is shown in Fig. 3. The molecular electrostatic potential (MEP) is useful for understanding and predicting the reactive behaviour of wide variety of chemical systems, in both electrophilic and nucleophilic reactions. The importance of MEP lies in the fact that it simultaneously displays molecular size, shape as well as positive, negative and neutral electrostatic potential regions in terms of colour grading and is very useful in research of molecular structure with its physiochemical property relationship. Molecular electrostatic potential (MEP) at a point around a molecule gives an indication of the net electrostatic effect produced at that point by total charge distributions (electron + nuclei) of the molecule and correlates with dipole moments, electronegativity, partial charges and chemical activity of the molecule. The different values of the electrostatic potential at the surface are represented by different colours. Potential increases in the order red < orange < yellow < green < blue where blue indicates the least repulsion attraction and red[1] indicates the strongest repulsion. It may be seen from Fig. 3 that the skeleton of the benzene ring shows more electrophilic region and the two methyl group attached to the benzene ring shows the zero potential region.

In MEPs, the maximum negative region, red in colour, indicates the preferred site for electrophilic attack while the blue coloured positive region indicates the nucleophilic attack.

Analysis of IR and Raman spectra

The title molecule has 21 atoms and belongs to the Cs point group symmetry. The 57 fundamental modes of vibrations of cumene are distributed using the relation Γvib = 39A′ + 18A″ into 39 in plane vibrations and 18 out of plane vibrations. The vibrational frequencies calculated at HF, B3LYP and B3PW91 methods with 6-31+/6-311++G(d,p) basis set along with observed FT-IR and FT-Raman frequencies for various modes of vibrations are presented in Table 2. The observed and simulated infrared and Raman spectra of cumene are shown in Figs. 4 and 5. The calculated frequencies are scaled down to give up the rational with the observed frequencies.

C—H vibrations

The C—H stretching vibrations are normally observed in the region 3100–3000 cm^{-1} for aromatic benzene structure [10,11]

[1] For interpretation of color in Fig. 3, the reader is referred to the web version of this article.

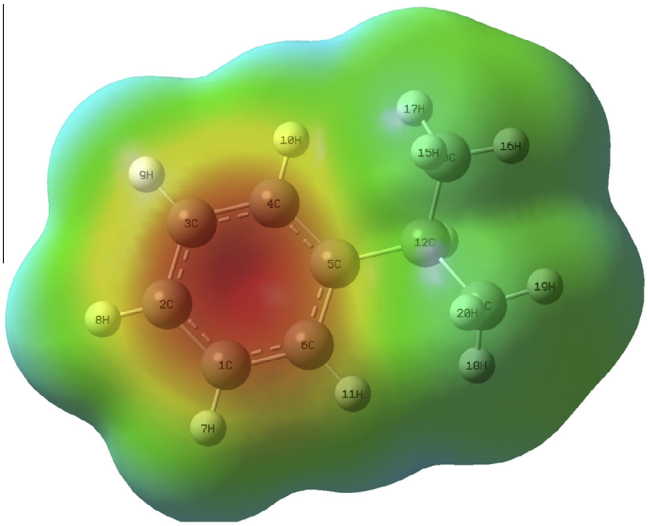

Fig. 3. Molecular electrostatic potential of cumene.

which shows their uniqueness of the skeletal vibrations. The very strong bands appeared at 3090, 3070, 3060, 3040 and 3030 cm^{-1} in the isopropyl benzene have been assigned to C—H ring stretching vibrations. The C—H ring stretching vibrations are found to be in the expected region which indicates that the C—H vibrations are not affected by the di-methyl substitution group.

C—H in-plane ring bending vibrations normally occur as a number of strong to weak intensity sharp bands in the region 1300–1000 cm^{-1} [12,13]. Ring C—H in-plane bending vibrations of the present compound are identified at medium to weak bands at 1300, 1290, 1280, 1210 and 1180 cm^{-1}. These C—H in-plane ring bending vibrations are observed at the expected region which indicate that these vibrations are not affected by substitution methyl group in the molecule.

The C—H out-of-plane bending vibrations are normally observed in the region 1000–800 cm^{-1} [14]. Ring C—H out of plane bending vibrations in the present case is observed at 1020, 1000, 960, 920 and 900 cm^{-1}, of which one is slightly above and rest are within the expected range. This may be due to the impact of methyl group attached to the benzene ring. After scaling procedure, the theoretical C—H vibrations are in good agreement with the experimental values.

Methyl groups vibrations

The methyl group vibrations are expected in the region of 3000–2900 cm^{-1} [10,11]. In the present molecule, the strong and very strong seven bands are observed at 2990, 2980, 2970, 2960, 2940, 2920 and 2870 cm^{-1}. These methyl C—H stretching vibrations are found to be well within the expected range which indicates the influence of the substitution over the skeletal vibrations are very less.

The C—H in-plane and out of plane are expected in the region 1250–1000 cm^{-1} and 950–720 cm^{-1} [14]. C—H in-plane bending vibrations of the present compound are 1160, 1150, 1140, 1110, 1080, 1050 and 1030 cm^{-1}. The C—H in-plane bending vibrations of the methyl group are observed at the lower region of the expected range. This may be due to the influence of skeletal vibration which suppress the methyl group vibrations. The C—H out-of-plane bending vibrations of methyl groups are observed at 850, 760, 750, 700, 650, 570 and 530 cm^{-1}, which are again slightly below the expected range and may be due to the impact of ring skeletal vibrations as in the case other CH vibrations.

Table 2
Observed and HF and DFT (B3LYP & B3PW91) with 6-311+G(d,p) level calculated vibrational frequencies of isopropyl benzene.

Sl. no.	Symmetry species	Observed frequency		HF/6-311+G(d,p)		B3LYP/6-311+G(d,p)		B3PW91/6-311+G(d,p)		PED % and vibration assignment
	C_S	FT-IR	FT Raman	(Calculated)	(Scaled)	(Calculated)	(Scaled)	(Calculated)	(Scaled)	
1	A′	3090 vs		3390	3102	3215	3096	3224	3088	γ CH (96%)
2	A′	3070 vs	3070 s	3388	3101	3213	3094	3221	3085	γ CH (91%)
3	A′		3060 vs	3366	3081	3200	3081	3211	3076	γ CH (93%)
4	A′	3040 s		3348	3065	3184	3066	3196	3061	γ CH (92%)
5	A′	3030 s		3338	3055	3175	3058	3187	3053	γ CH (93%)
6	A′	2990 s		3262	3011	3116	3001	3134	3002	γ CH (85%)
7	A′	2980 vs		3259	3008	3114	2999	3133	3001	γ CH (84%)
8	A′	2970 vs	2970 m	3251	3001	3109	2994	3128	2997	γ CH (84%)
9	A′	2960 vs		3240	2991	3103	2988	3124	3009	γ CH (86%)
10	A′	2940 vs	2940 m	3187	2942	3041	2929	3051	2939	γ CH (94%)
11	A′	2920 vs		3180	2901	3037	2924	3047	2935	γ CH (97%)
12	A′	2870 vs		3153	2876	2991	2861	3007	2867	γ CH (92%)
13	A′	1800 w		1798	1785	1651	1824	1664	1782	γ CC (65%) + γ HCC (20%)
14	A′	1750 w		1767	1755	1627	1744	1640	1756	γ CC (68%) + γ HCC (12%)
15	A′	1660 vs		1665	1654	1537	1647	1537	1646	γ CC (47%) + HCC (19%)
16	A′		1610 m	1646	1634	1524	1634	1520	1628	γ CC (25%) + HCC (20%)
17	A′	1600 vs		1627	1598	1505	1614	1500	1596	γ HCC (65%)
18	A′		1580 vw	1624	1595	1504	1595	1498	1594	γ HCC (75%)
19	A′	1520 w		1611	1507	1492	1527	1487	1506	γ HCC (71%) + HCH (10%)
20	A′	1490 m		1598	1494	1478	1494	1478	1382	γ CC (46%) + HCC (26%)
21	A′	1470 m	1470 w	1554	1470	1428	1487	1421	1484	γ HCC (96%)
22	A″		1450 w	1537	1454	1408	1466	1402	1464	β CH (88%)
23	A″	1390 vs		1477	1398	1362	1393	1373	1386	β HCC (66%)
24	A″	1370 vs		1465	1386	1350	1381	1347	1360	β HCC (42%)
25	A″	1330 m		1454	1376	1336	1350	1334	1347	β HCC (57%)
26	A″		1310 vw	1331	1286	1315	1315	1316	1329	β HCC (41%)
27	A′	1300 m		1326	1281	1227	1277	1231	1286	β HCC (47%) + β CC (22%)
28	A′		1290 vw	1310	1286	1218	1287	1215	1276	ββ HCC (73%) + CC (22%)
29	A′	1280 m		1257	1234	1185	1253	1183	1244	β HCC (79%) + CC (15%)
30	A′	1210 w	1210 s	1239	1216	1159	1186	1158	1202	β HCH (79%) + HCC (40%)
31	A′	1180 w	1180 w	1201	1179	1146	1193	1153	1196	β HCH (48%) + HCC (26%)
32	A′		1160 w	1185	1163	1092	1136	1097	1139	β HCC (13%) + CC (50%)
33	A′	1150 w		1168	1179	1090	1164	1089	1170	β CC (59%)
34	A′	1140 w		1125	1135	1052	1123	1057	1135	β CC (80%)
35	A′	1110 m	1110 vw	1122	1102	1014	1082	1013	1070	β CC (56%) + CCC (13%)
36	A′	1080 s	1080 vw	1103	1083	1000	1066	999	1055	β CC (79%)
37	A′	1050 vs		1086	1031	981	1046	981	1035	HCC (82%) + CCCC (11%)
38	A′		1030 vw	1043	991	970	1036	971	1026	δ HCH (40%)
39	A″	1020 vs		1026	1007	927	1025	924	1018	δ HCH (13%)
40	A″		1000 vs	1002	1025	921	1016	920	1012	δ HCCC (79%)
41	A″		960 vw	950	973	889	982	899	990	δ HCC (40%) + CCC (33%)
42	A″	920 m		947	929	853	942	852	921	δ HCC (63%)
43	A″	900 s		848	868	773	855	773	836	δ HCCC (97%)
44	A″		850 vw	787	806	734	812	737	812	δ HCC (63%) + CC (40%)
45	A″	760 s		770	740	708	733	707	733	δ HCC (37%) + CC (38%)
46	A″		750 w	679	652	634	675	630	654	δ HCCC (87%)
47	A″	700 vs		629	648	583	644	580	639	δ HCCC (37%) + CC (13%)
48	A″	650 s		526	542	489	540	488	537	δ HCCC (36%) + CCC (47%)
49	A″	570 m	570 vw	450	464	420	464	420	496	δ CC (76%)
50	A″	530 vs		447	502	413	502	410	501	δ CCC (74%)
51	A′	400 w		442	495	409	496	406	455	δ CC (34%) + CCC (44%)
52	A′		320 vw	388	372	360	398	359	391	β CC (17%) + HCC (14%)
53	A′	310 m	310 w	294	301	268	296	266	289	β CCC (57%) + HCC (27%)
54	A′	250 m		274	269	252	278	250	272	β CCC (58%) + HCC (25%)
55	A′		150 w	219	340	207	321	205	317	δ CCC (13%) + HCCC (69%)
56	A″		140 w	160	248	145	226	144	224	δ CCCC (87%)
57	A″	70 m	70 s	68	106	62	96	62	97	δ CCCC (92%)

γ – stretching; β – in-plane bending; δ – out-of-plane bending; vs – very strong; s – strong; m – medium; w – weak; vw – very weak.

For methyl substituted benzene derivatives, the anti-symmetric and symmetric deformation vibrations of methyl group normally occur in the region 1465–1440 cm^{-1} and 1390–1370 cm^{-1}, respectively [15]. The wave number at 1450 and 1390 cm^{-1} in FT-IR and Raman is assigned to CH_3 scissoring vibration. The wave number 1370 cm^{-1} in FT-IR is assigned to CH_3 wagging vibration. The rocking mode of the CH_3 group is assigned at 1330 cm^{-1}. The twisting mode of the CH_3 group is observed at 1310 cm^{-1} (Raman) and torsion vibration is identified below 500 cm^{-1}. These values have been tuned to assign with reference to work done in earlier paper [16].

Ring vibrations

The ring stretching vibrations are expected within the region 1620–1390 cm^{-1} [17]. Most of the ring modes are altered by the substitution to aromatic ring. The bands due the C=C stretching vibrations are normally observed in the region 1625–1575 cm^{-1} [10,11]. In the present case C=C stretching vibrations are observed at 1800, 1750 and 1660 cm^{-1} which is clearly above the expected range. This increase in wavenumbers is due to the substitution of the propyl group attached to phenyl ring.

The bands due the C—C stretching vibrations are called skeletal vibrations normally observed in the region 1430–1575 $cm^{-1}$for the

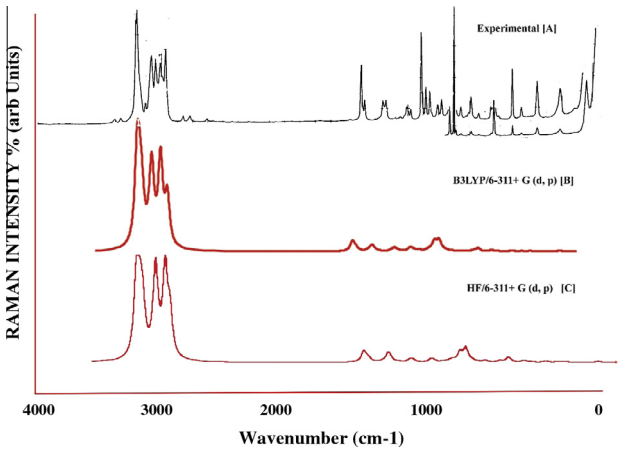

Fig. 4. Experimental and calculated FT-Raman spectrum of cumene.

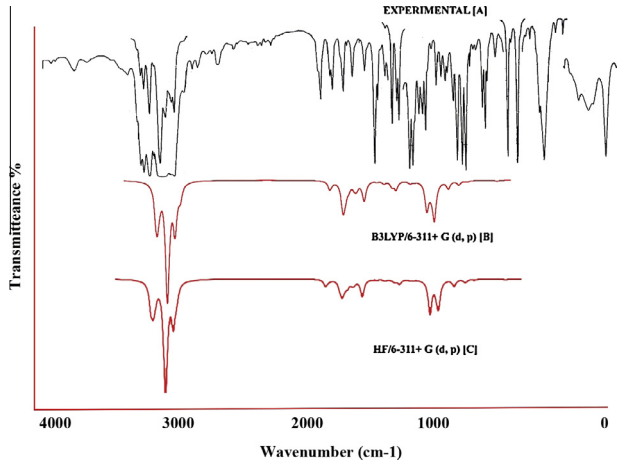

Fig. 5. Experimental and calculated FT-IR spectrum of cumene.

aromatic ring compounds. In the present case the C—C stretching vibrations are observed at 1610, 1600, 1580, 1520, 1490 and 1470 cm^{-1}. The C—C stretching vibration is observed slightly above the expected range which may be due to the impact of di-methyl substitution group. It is observed that both C=C and C—C are much affected by the substitutional group.

Thermodynamic properties

The values of some of the thermodynamic parameters; specific heat capacity, entropy, and enthalpy of cumene in ground state are calculated using B3LYP methods with 6-31+G(d,p) basis set and values are listed in Table. 3. It can be observed from Table 4 and Fig. 6. The thermodynamic functions are increasing with increase in temperature which may be due to the fact that the molecular vibrational intensities increase with temperature. All the thermodynamic calculations were done in gas phase. Kishimoto et al. [23] have measured the heat capacity with an adiabatic colorimeter for a crystal from 14 to 177.13 K, for the glassy state from 14 to 126 K (glass transition temperature: *Tg*) and for the liquid from *Tg* to 313 K, with a sample of 99.93% purity. From the study it is observed that there is linear increase of the thermodynamical properties to the increase of the temperature. The same characteristics are also observed in the present study. At the same time, the values of thermodynamical parameters, namely, heat capacity, enthalpy and entropy obtained by different phases of the

Table 3
Thermodynamic properties at different temperatures at the B3LYP/6-311++G(d,p) level of cumene.

^{a}T (K)	$C^{0}_{p,m}$ (cal mol^{-1} K^{-1} ^{a})	S^{0}_{m} (cal mol^{-1} K^{-1} ^{a})	ΔH^{0}_{m} (kcal mol^{-1} ^{a})
100	9.50	62.27	117.48
150	13.46	67.64	118.05
200	18.29	72.73	118.84
250	23.76	77.83	119.89
300	29.60	83.04	121.22
350	35.46	88.35	122.85
400	41.07	93.72	124.76
450	46.27	99.10	126.95
500	51.00	104.43	129.38
550	55.28	109.68	132.04
600	59.13	114.83	134.90
650	58.91	113.35	142.81
700	68.64	129.54	144.52

[a] *T*: temperature; *C*: heat capacity; *S*: entropy; *H*: enthalpy.

Table 4
The electronic dipole moment (μ) (Debye), polarizability (α) and first hyperpolarizability (β) of cumene.

Parameter	a.u.	Parameter	a.u.
α_{xx}	−59.3546	β_{xxx}	0.8747
α_{xy}	1.5461	β_{xyy}	−2.1231
α_{yy}	−53.2337	β_{xzz}	1.0085
α_{xz}	0.0000	β_{yyy}	7.4267
α_{yz}	0.0000	β_{yxx}	7.3553
α_{zz}	−53.0152	β_{yzz}	−5.4195
α_{tot}	−55.2012	β_{zzz}	0.0000
$\Delta\alpha$	3.34204×10^{-24} esu	β_{yyz}	0.0000
μ_x	0.1210	β_{xxz}	0.0000
μ_y	0.4462	β_{tot}	49.03×10^{-33} esu
μ_z	0.0000		
μ_{tot}	0.4623 D		

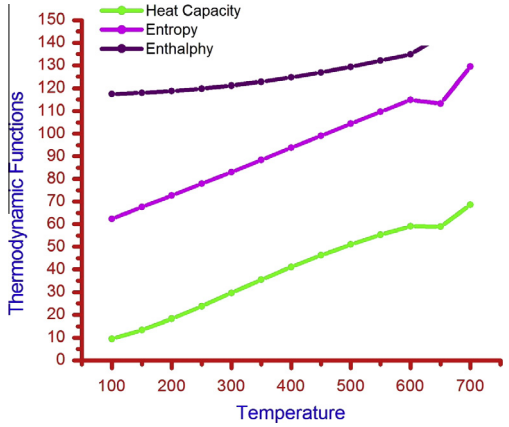

Fig. 6. Thermodynamical graphs of cumene.

compound in experimental, are very high to the corresponding temperature when compared to the present study with quantum computational methods. The experimental values of the cumene studied in glass state for the heat capacity, entropy and enthalpy in 100 K are 78.20, 78.53 and 42.44 J K^{-1} mol^{-1} respectively, whereas the values obtained for the same parameters by DFT method using B3LYP functional with 6-311+G(d,p) basis set, are 9.5, 62.27 and 117.78 J K^{-1} mol^{-1} respectively. The quantum computational methods have to be refined more with correlations to elucidate closer approximate values of thermodynamical parameters.

NLO property

In order to find the relationships among molecular structures and non-linear optic properties (NLO), the polarizabilities and first order hyperpolarizabilities of the isopropyl benzene compound were calculated using B3LYP method with 6-31++G(d,p) basis set. The calculations of the total molecular dipole moment (μ), linear polarizability (α), the first-order hyperpolarizability (β) indicate the non-linear optical property of the molecule [18–22], the calculated values are presented in Table 4. The equations used for calculating the magnitude of total dipole moment μ, the mean polarizability (α_0) and the anisotropic polarizabilities $\Delta\alpha$ and <β> are based on the previous works [24].

It is well known that the higher values of dipole moment, molecular polarizability, and hyperpolarizability are important for more active NLO properties. The calculated values of dipole moment, polarizability (α) and hyperpolarizability (β) are 0.4623 Debye, 3.34204×10^{-24} esu and 49.03×10^{-33} esu. From these values the dipole moment (μ) and hyperpolarizability (β) are much lower than that of urea (μ and β of urea are 1.3732 D and 372.89×10^{-33} esu) [25]. Based on the calculated values the cumene can least be considered for NLO material.

Ultraviolet spectra and frontier molecular analysis

The electronic property arises from the transfer of electron of molecule from π or non-bonding to the ant bonding or excited states of the energy levels. The common type of the electronic transitions in organic compounds is π–π^*, n–π^* and π^* (acceptor) and π (donor). In the present molecule electronic characteristics are performed in TD-SCF functional using B3LYP method with 6-311+G(d,p) basis set. The contribution of the charge from HOMO-to LUMO is calculated from the Gauss sum 2.2 free software and the values of maximum wavelength, oscillator strength and excitation energies are presented in Table 5. The pictorial form of the HOMO and LUMO charge transfer is shown in Fig. 7.

The absorption maxima due to electron transition in gas phase are found to be at 214.83, 213.39, 181.20 nm. The oscillator strengths for the corresponding transitions are 0.0035, 0.0032, and 0.0169, respectively. The maximum energy gap observed is 6.84 eV. In the case of ethanol, maximum are 214.38, 213.86 and 179.60 nm, oscillator strength 0.0059, 0.0037 and 0.0419 and maximum energy gap 6.9 eV respectively. In methanol solvent, they are 214.34, 213.75, 179.53 nm; oscillator strength 0.0057, 0.0037, 0.0390 and maximum energy 6.9 eV respectively. They are all assigned to the transitions $\pi \rightarrow \pi^*$ which is also confirmed in NBO analysis. It is worth mentioning that for the cumene molecule, all the three parameters; the absorption maximum, excitation energy and oscillator strength are almost equal in all the three phases.

The energies of HOMO and LUMO, Kubo gap, electronegativity, chemical hardness, global softness and electrophilicity index are calculated and presented in Table 6. The average chemical hardness from gas to solvent phase is 5.40 eV which considerably high and hence the compound is chemically stable. Similarly, the electro negativity is observed to be 3.4 eV. The electro negativity is a measure of attraction of an atom for electrons in a covalent bond. The candidate molecule has lower electronegativity, thus it does less charge flow occur. The electrophilicity index is a measure of energy lowering due to the maximal electron flow between the donor [HOMO] and the acceptor [LUMO]. From Table 7, it is found that the electrophilicity index of cumene is 1.07 eV in the gas phase and 1.09 eV in solvent, which is found very low, and this value ensures that there is very less energy transformation between HOMO and LUMO.

NBO analysis

NBO analysis provides the most accurate possible 'natural Lewis structure', because all orbital details are mathematically chosen to include the highest possible percentage of the electron density. A useful aspect of the NBO method is that it gives information about interactions in both filled and virtual orbital spaces that could enhance the analysis of intra- and intermolecular interactions. The NBO analysis of the cumene molecule was calculated by B3LYP method with 6-31+9(d,p) basis set. The calculated values are given in Table 7.

From the table it is clearly observed that there are $\pi \rightarrow \pi^*$ conjugation in the phenyl and its extension is not made out the ring but rather within the ring through $\pi_{C-C} \rightarrow \pi^*_{C-C}$ hyper conjugation. The pairs in the ring π_{C1-C6} show conjugation with π^*_{C2-C3} and π^*_{C4-C5} having the stabilization energy 19.52 and 20.47 kcal/mol respectively. Similarly π_{C2-C3} shows conjugation with π^*_{C1-C6} and π^*_{C4-C5} with the stabilization energy 20.77 and 19.23 kcal/mol. And in the same way π_{C4-C5} has conjugation with π^*_{C1-C6} and π^*_{C2-C3} with the stabilization energy 19.57 and 21.20 kcal/mol. Among this C1—C6 prefers to be acceptor than to be donor for it retain higher energy in place of the acceptor. All these highest probable transitions are observed only within the benzene ring.

NMR spectra analysis

NMR spectroscopy is currently used for structure elucidation of complex molecules. The optimized structure of isopropyl benzene

Table 5
Theoretical electronic absorption spectra of cumene (absorption wavelength λ (nm), excitation energies E (eV) and oscillator strengths (f)) using TD-DFT/B3LYP/6-31++G(d,p) method.

λ (nm)	E (eV)	(f)	Major contribution	Assignment	Region	Bands
Gas						
214.83	5.77	0.0035	H → L (20%)	$\pi \rightarrow \pi^*$	Quartz UV	R-band (German, radikalartig)
213.39	5.81	0.0032	H → L (20%)	$\pi \rightarrow \pi^*$	Quartz UV	
181.20	6.84	0.0169	H → L (100%)	$\pi \rightarrow \pi^*$	Quartz UV	
Ethanol						
214.38	5.78	0.0059	H → L (20%)	$\pi \rightarrow \pi^*$	Quartz UV	R-band (German, radikalartig)
213.86	5.79	0.0037	H → L (10%)	$\pi \rightarrow \pi^*$	Quartz UV	
179.60.	6.90	0.0419	H → L (100%)	$\pi \rightarrow \pi^*$	Quartz UV	
Methanol						
214.34	5.78	0.0057	H → L (15%)	$\pi \rightarrow \pi^*$	Quartz UV	R-band (German, radikalartig)
213.75	5.80	0.0037	H → L (10%)	$\pi \rightarrow \pi^*$	Quartz UV	
179.53	6.90	0.0390	H → L (100%)	$\pi \rightarrow \pi^*$	Quartz UV	

H: HOMO; L: LUMO.

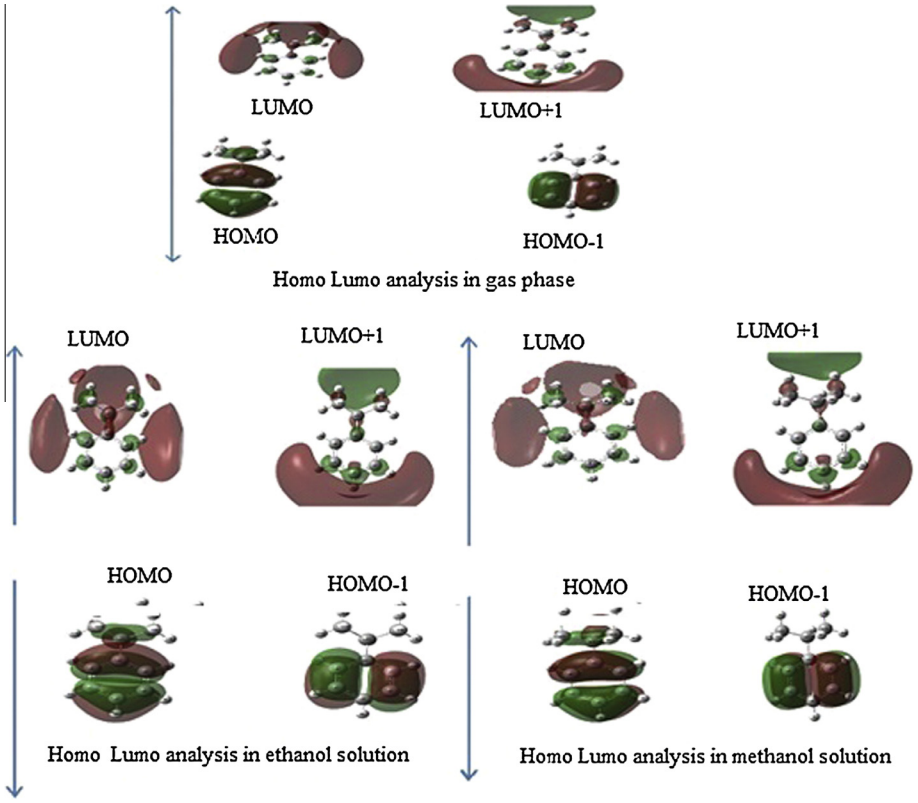

Fig. 7. Molecular orbitals and energies for the HOMO and LUMO of cumene.

Table 6
HOMO, LUMO, Kubo gap, global electronegativity, global hardness and softness, global electrophilicity index of cumene.

Parameters	Gas	Ethanol	Methanol
E_{HOMO} (eV)	−8.88	−8.90	−8.90
E_{LUMO} (eV)	1.94	2.02	2.02
$\Delta E_{HOMO-LUMO\ gap}$ (eV)	6.81	6.88	6.88
Electronegativity, χ (eV)	3.38	3.44	3.44
Chemical hardness, η (eV)	5.35	5.46	5.46
Global softness, σ (eV)	0.19	0.18	0.18
Electrophilicity index, ω (eV)	1.07	1.08	1.09
Dipole moment, μ (Debye)	0.47	0.66	0.66

is used to calculate the NMR spectra at B3LYP method with 6-31++G(2d,p) basis set using the GIAO method. The chemical shifts of the compound are calculated with reference to TMS for the atoms ^{1}H and ^{13}C and values are presented in Table 8 In the case of isopropyl benzene, the chemical shift of the substitutional groups is C12, C13, and C14 are 6.411, −0.631 and −0.631 ppm respectively. The chemical shifts of the carbons are completed shielded by the surrounding hydrogen atoms, especially the carbon two carbon atoms of the methyl group are shield to the extent of lower than the TMS reference line. The aromatic carbon atoms generally give rise to signals in the range of 100–150 ppm V. Karunakaran and Balachandran [26] have found the aromatic carbons shielding in 4-methyl propiophenone between the range 130–140 ppm. In the present compound the six aromatic carbons too observed in the expected range. Among six carbon atoms of the aromatic ring, C5 found to be 130 ppm, at which the substitutional group is attached.

Usually the hydrogen atom shows the chemical shifts below 10 ppm. In the present compound too all the hydrogen atoms attached to phenyl rings are around 7 ppm. The hydrogen atoms

Table 8
Calculated ^{1}H and ^{13}C NMR and chemical shifts (ppm) of cumene.

Atoms	Gas	Solvent Acetone
	TMS B3LYP/6-311+G(2d,p) shift	TMS B3LYP/6-311+G(2d,p) shift
5C	130.32	131.48
1C	111.1	111.18
2C	106.63	106.35
3C	111.1	111.18
4C	107.18	107.43
6C	107.18	107.43
12C	6.284	6.411
13C	−0.3434	−0.631
14C	−0.3434	−0.639
10H	7.779	7.965
11H	7.779	7.965
9H	7.438	7.612
7H	7.438	7.612
8H	7.19	7.340
21H	1.758	1.826
17H	1.355	1.423
18H	1.355	1.423
16H	0.344	0.421
19H	0.344	0.421
15H	−0.071	−0.121
20H	−0.071	−0.121

of the substitutional show very closer to the TMS reference line and among this the methyl hydrogen atoms are observed blow the reference line. This trend is observed in the literature [25].

Conclusion

A complete vibrational analysis, thermodynamic properties, HOMO and LUMO analysis, NLO properties, NBO analysis and UV–Vis spectral analysis of isopropyl benzene are by performed

HF and DFT-B3LYP methods with 6-31++G(d,p) basis sets. The influences of -methyl group and benzene ring on the vibrational frequencies of the title compound were discussed. The calculated values are scaled to rationalize the observed values. From potential energy surface scan (PES) study the results show that cumene molecule have three possible structures at global minimum energy, depending on the positions of the methyl group bonded to benzene ring.

The molecular electrostatic potential (MEP) map is performed and the skeleton of the benzene ring shows more electrophilic region at the place of atom where substitutional group is attached. From the UV–Visible spectra, it is found that the present compound is not optically active and do not possess NLO properties. There is less possibility of the charge transfer from HOMO to LUMO. From NBO analysis the three possible conjugations of the π are found only within the ring and there is no extension of conjugation to the substitutional group for it does not possess π-bonds.

Furthermore, the thermodynamic properties of the compounds have been calculated. It was seen that the heat capacities, entropies and enthalpies increase with the increasing temperature. The chemical shifts of the compound are computed. The aromatic carbon atoms are found within the expected range and carbons atoms of the substitutional group are found completely shielded. Similarly the hydrogen atoms attached to phenyl ring are observed in the range and chemical shift of the hydrogen atoms attached to methyl is found below the TMS reference line.

Acknowledgements

We remain grateful to the Administration of St. Joseph's College of Arts and Science (Autonomous), Cuddalore for providing us the Quantum Computational Research Lab for all the computational works of the compound.

Appendix A. Supplementary material

Supplementary data associated with this article can be found, in the online version, at http://dx.doi.org/10.1016/j.molstruc.2014.11.035.

References

[1] J.F. Knifton, US Pat., 4870217, 1989 (assigned to Texaco Chemical Company).
[2] Reid Sherwood, Properties of Gases and Liquids, pages: 149, 203, 204.
[3] J.I. Seeman, H.V. Secor, P.J. Breen, V.H. Grassian, E.R. Brenstein, J. Am. Chem. Soc. 111 (1989) 3140.
[4] J.B. Lagowski, I.G. Csizmadia, G.J. Vancso, J. Mol. Struct. (Theochem.) 258 (1992) 341.
[5] T. Schaefer, R. Sebastian, G.H. Penner, Can. J. Chem. 66 (1988) 1495.
[6] R.J. Lewis Sr. (Ed.), Hawley's Condensed Chemical Dictionary, 12th ed., Van Nostrand Rheinhold Co., New York, NY, 1993. p. 860.
[7] W. Gerhartz, Ullmann's Encyclopedia of Industrial Chemistry, fifth ed., VCH Publishers, Deerfield Beach, FL, 1985. p. 21.
[8] S. Xavier et al., Spectrochim. Acta Part A Mol. Biomol. Spectrosc. 137 (2015) 306–320.
[9] A.I. Fishmana, A.I. Noskova, A.B. Remizovb, D.V. Chachkovb, Spectrochim. Acta Part A Mol. Biomol. Spectrosc. 71 (2008) 1128–1133.
[10] Y.R. Sharma, Elementary Organic Spectroscopy, Principles and Chemical Applications, S. Chande & Company Ltd., New Delhi, 1994. pp. 92–93.
[11] P.S. Kalsi, Spectroscopy of Organic Compounds, Wiley Eastern Limited, New Delhi, 1993.
[12] G. Socrates, Infrared and Raman Characteristic Group Frequencies – Tables and Charts, third ed., Wiley, New York, 2001.
[13] F.R. Dollish, W.G. Fateley, F.F. Bentley, Characteristic Raman Frequencies of Organic Compounds, Wiley, New York, 1997.
[14] G. Varsanyi, Vibrational Spectra of Benzene Derivatives, Academic Press, New York, 1969.
[15] G. Varsanyi, Assignments of Vibrational Spectra of 700 Benzene Derivatives, Wiley, New York, 1974.
[16] A. Altun, K. Golcuk, M. Kumru, J. Mol. Struct. (Theochem.) 625 (2003) 17–24.
[17] R.L. Peesole, L.D. Shield, I.C. McWilliam, Modern Methods of Chemical Analysis, Wiley, New York, 1976.
[18] A.B. Ahmed, H. Feki, Y. Abid, H. Boughzala, C. Minot, A. Mlayah, J. Mol. Struct. 920 (2009) 1.
[19] J.P. Abraham, D. Sajan, V. Shettigar, S.M. Dharmaprakash, I. Nemec, I.H. Joe, V.S. Jayakumar, J. Mol. Struct. 917 (2009) 27.
[20] S.G. Sagdinc, A. Esme, Spectrochim. Acta Part A 75 (2010) 1370.
[21] A.B. Ahmed, H. Feki, Y. Abid, H. Boughzala, C. Minot, Spectrochim. Acta Part A 75 (2010) 293.
[22] S. Xavier, S. Ramalingam, S. Periandy, Experimental [FT-IR and FT-Raman] analysis and theoretical [IR, Raman, NMR and UV–Visible] investigation on propylbenzene, J. Theor. Comput. Sci. 1 (2014) 109.
[23] Koji Kishimoto, Hiroshi Suga, Syuzo Seki, Bull. Chem. Soc. Jpn. 46 (1973) 3020–3031.
[24] I. Fleming, Frontier Orbitals and Organic Chemical Reactions, Wiley, London, 1976.
[25] Y.X. Sun, Q.I. Hao, W.X. Wei, Z.X. Yu, I.D. Lu, X. Wang, Y.X. Wang, J. MOL. Struct. THEOCHEM 904 (2009) 74–82.
[26] V. Karunakaran, V. Balachandran, Spectrochim. Acta Part A: Mol. Biomol. Spectrosc. 128 (2014) 1–14.